Meteor Trajectory from Multiple Station Head Echo Doppler Observations

Christian Steyaert [1], Felix Verbelen [2], and the VVS Beacon Observers [3]

An improved method for determining a meteor's trajectory from its head echo Doppler signature is presented. This methodology is derived from pioneering work from over half a century ago. The new analytical technique employs head echo data that was simultaneously captured by multiple receiving stations located around a low power beacon. In addition to the geometrical data, Monte Carlo simulations of timing errors were generated and reviewed. The method shows great potential, especially if tighter constraints in the inter-station timing can be achieved.

Received 2010 May 25

1 Introduction

Manning (Manning et al., 1949) pioneered Doppler observations of head echoes to determine meteor heights and velocities. With the growing use of pulsed backscatter radar providing more precise data their technique was soon abandoned. Decades later Richardson and Kuneth (1998) revived meteor trajectory determinations using head echo observations. They used both a long base (Richardson) and medium base line (Kuneth) forward scatter reflections from AM modulated video carriers. Their revised method called for additional assumptions including standard range and assumed path geometry of the reflections.

In this article we extend Richardson's and Kuneth's method and apply it to relatively short range observations obtained from the VVS's low powered continuous wave (CW) beacon. We also discuss the limitations of the method as well as possible improvements to the setup and observations.

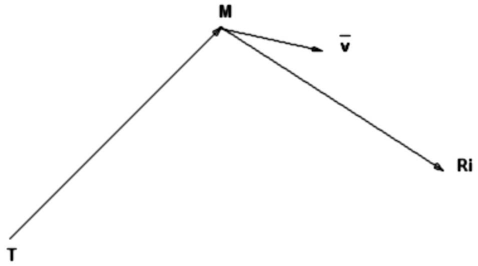

Figure 1 – Head echo geometry.

2 The CW beacon and the receiving stations

The description of the 50 W, CW, beacon at Zillebeke (near Ypres), Belgium is extensively described in (Steyaert, 2006). It has been operating with minimal downtime since April 2005.

The beacon's frequency of 49.990 MHz was consciously chosen to fall just below the six meter ham band to avoid interference during sporadic E and other types of strong propagation band openings. As a result of this frequency choice only specialized, and therefore pricy, receivers can tune to this frequency. Since it was felt the expense of such specialized receivers would limit the number of potential observers, the Working Group Radio Astronomy of the VVS placed a group order for twenty fixed frequency, ready to use, receivers. The receivers, model MRX-50, are produced by AITEC of Japan. The receivers were imported early in 2008. AITEC also manufacturers the HRO receivers used in the Japanese beacon project, AMRO, which is headed by Kimio Maegawa (AMRO, 2010).

In addition to the currently operational stations using the VVS's beacon there are several stations still under construction that will use the remaining MRX-50 receivers and others that will use a different receiver.

Typically forward scatter radio meteor observers use software that records spectrograms continuously, although a few stations record only during the periods of the larger streams.

For the head echo study an additional step is required; the audio signal needs to be recorded as well. The recordings are normally in the `.wav` format. The principle and potential yield of head echo observations from several locations was outlined in project 'HADES' (Steyaert & Verbelen, 2006).

3 The Method

Consider the transmitter T, instantaneous meteor head position M with velocity vector $\bar{v}$, and receiver R_i.

The corresponding Cartesian coordinates are:

$$\begin{aligned} TM_x &= (x_M - x_T) \\ TM_y &= (y_M - y_T) \\ TM_z &= (z_M - z_T) \end{aligned} \quad (1)$$

[1] Vereniging voor Sterrenkunde (VVS), Belgium.
Email: `steyaert@vvs.be`
[2] Volkssterrenwacht Mira, Belgium.
Email: `felix.verbelen@skynet.be`

[3] Janos Barabas, Rik Blondeel, Willy Camps, Johan Coussens, Edwin De Ceuninck, Gaspard De Wilde, Franky Dubois, Pierre Ernotte, Association Jonckheere (test), Volkssterrenwacht Mira (demo), Roland Oeyen, Lucas Pellens, Roger Segers, Chris Steyaert, Dirk Van Hessche, Maarten Vanleenhove, Patrick Vanouplines (TV), Felix Verbelen, John Wardle, Joseph Welkenhuyzen

IMO bibcode WGN-384-steyaert-trajectory
NASA-ADS bibcode 2010JIMO...38..119S

$$
\begin{aligned}
R_iM_x &= (x_M - x_{Ri}) \\
R_iM_y &= (y_M - y_{Ri}) \\
R_iM_z &= (z_M - z_{Ri})
\end{aligned} \tag{2}
$$

3.1 Instantaneous Doppler shift

The Doppler shift for receiver 'i' is the sum of two parts

$$Doppl_i = Doppl_T + Doppl_{Ri} \tag{3}$$

with $Doppl_T$ the Doppler shift from the transmitter to the meteor, and $Doppl_{Ri}$ the Doppler shift from the meteor to the receiver 'i'.

The radial velocity component that contributes to the Doppler shift is conveniently obtained by means of the scalar product of the direction vector and the velocity vector:

$$Doppl_T = -\frac{\overline{TM}}{|\overline{TM}|} \cdot \frac{\overline{v}}{c} f \tag{4}$$

$$Doppl_{R_i} = -\frac{\overline{R_iM}}{|\overline{R_iM}|} \cdot \frac{\overline{v}}{c} f \tag{5}$$

with the lengths:

$$|\overline{TM}| = \sqrt{TM_x^2 + TM_y^2 + TM_z^2} \tag{6}$$

$$|\overline{R_iM}| = \sqrt{R_iM_x^2 + R_iM_y^2 + R_iM_z^2} \tag{7}$$

and c the speed of light, f the frequency.

Expanding (4) and (5) in coordinates gives:

$$Doppl_T = -\frac{(TM_xv_x + TM_yv_y + TM_zv_z)}{\sqrt{TM_x^2 + TM_y^2 + TM_z^2}} \frac{f}{c} \tag{8}$$

$$Doppl_{Ri} = -\frac{(R_iM_xv_x + R_iM_yv_y + R_iM_zv_z)}{\sqrt{R_iM_x^2 + R_iM_y^2 + R_iM_z^2}} \frac{f}{c} \tag{9}$$

and for the total $Doppl_i$:

$$
\begin{aligned}
Doppl_i = \\
-\frac{f}{c}\left(\frac{TM_x}{\sqrt{TM_x^2+TM_y^2+TM_z^2}} + \frac{R_iM_x}{\sqrt{R_iM_x^2+R_iM_y^2+R_iM_z^2}}\right) v_x \\
-\frac{f}{c}\left(\frac{TM_y}{\sqrt{TM_x^2+TM_y^2+TM_z^2}} + \frac{R_iM_y}{\sqrt{R_iM_x^2+R_iM_y^2+R_iM_z^2}}\right) v_y \\
-\frac{f}{c}\left(\frac{TM_z}{\sqrt{TM_x^2+TM_y^2+TM_z^2}} + \frac{R_iM_z}{\sqrt{R_iM_x^2+R_iM_y^2+R_iM_z^2}}\right) v_z
\end{aligned} \tag{10}
$$

this can be rewritten as:

$$Doppl_i = A_iv_x + B_iv_y + C_iv_z \tag{11}$$

Scalars A_i, B_i, C_i are the only function of the position of the meteor. Hence velocity components v_x, v_y, v_z can be obtained from solving the linear system

$$
\begin{bmatrix}
\sum_i A_i^2 & \sum_i A_iB_i & \sum_{A_iC_i} \\
\sum_i A_iB_i & \sum_i B_i^2 & \sum_{B_iC_i} \\
\sum_{A_iC_i} & \sum_{B_iC_i} & \sum_i C_i^2
\end{bmatrix}
\begin{bmatrix} v_x \\ v_y \\ v_z \end{bmatrix} =
= \begin{bmatrix}
\sum_i Doppl_{Obsi}A_i \\
\sum_i Doppl_{Obsi}B_i \\
\sum_i Doppl_{Obsi}C_i
\end{bmatrix} \tag{12}
$$

from the Doppler shift observations of at least three different locations.

Linear system (12) is the solution of the least square form:

$$Min\frac{1}{2}\sum_i (Doppl_{Obsi} - A_iv_x - B_iv_y - C_iv_z)^2 \tag{13}$$

with respect to the velocity components v_x, v_y, v_z.

3.2 Doppler shift derivative

Similar to the Doppler shift itself, the derivative or slope of the Doppler shift for receiver 'i' is the sum of two parts:

$$\frac{\partial Doppl_i}{\partial t} = \frac{\partial Doppl_T}{\partial t} + \frac{\partial Doppl_{R_I}}{\partial t} \tag{14}$$

Assuming a time independent velocity vector $\overline{v}$

$$\frac{\partial Doppl_T(t)}{\partial t} = -\frac{1}{|\overline{TM}|}\left[v^2 - \frac{\left(\overline{TM}\cdot\overline{v}\right)^2}{TM^2}\right]\frac{f}{c} \tag{15}$$

$$\frac{\partial Doppl R_i(t)}{\partial t} = -\frac{1}{|\overline{R_iM}|}\left[v^2 - \frac{\left(\overline{R_iM}\cdot\overline{v}\right)^2}{R_iM^2}\right]\frac{f}{c} \tag{16}$$

with

$$TM^2 = |\overline{TM}|^2 = TM_x^2 + TM_y^2 + TM_z^2 \tag{17}$$

$$R_iM^2 = |\overline{R_iM}|^2 = R_iM_x^2 + R_iM_y^2 + R_iM_z^2 \tag{18}$$

$$v^2 = \overline{v}^2 = \overline{v}.\overline{v} = v_x^2 + v_y^2 + v_z^2 \tag{19}$$

3.3 Solving the equations

The goal is to find the position, M, and velocity vector, $\overline{v}$, from the observed Doppler shifts and Doppler shift derivatives at a given time.

The six unknowns x_M, y_M, z_M and v_x, v_y, v_z can in principle be obtained from at least three $Doppl_{Obsi}$ and the corresponding $\frac{\partial Doppl_{Obsi}}{\partial t}$. The general procedure is:

- choose M (x_M, y_M, z_M)
- solve (12) for v_x, v_y, v_z
- calculate for each 'i ' $\frac{\partial Doppl_i}{\partial t}$ with (12)
- calculate $J = \frac{1}{2}\sum_i\left(\frac{\partial Doppl_i}{\partial t} - \frac{\partial Doppl_{Obsi}}{\partial t}\right)^2$ (20)
- iterate M for minimum value J

In case of a stream meteor, the velocity vector is fairly well known so the following alternative procedure can be used:

- choose M (x_M, y_M, z_M)
- calculate for each 'i '$Doppl_i$ with (10)
- calculate $J' = \frac{1}{2}\sum_i (Doppl_i - Doppl_{Obsi})^2$ (21)
- calculate for each 'i '$\frac{\partial Doppl_i}{\partial t}$ with (12)
- calculate $J = \frac{1}{2}\sum_i \left(\frac{\partial Doppl_i}{\partial t} - \frac{\partial Doppl_{Obsi}}{\partial t}\right)^2$ (20)
- iterate M for minimum value $J + \lambda J'$ (22)

λ is a positive weight factor.

3.4 Measurements at different absolute times

In section 3.3 we stated loosely that the time of all measurements was equal. However this is not a necessary condition. If at time t = 0 the coordinates of the head echo are $x_M; y_M; z_M$, then they are at time t_i :

$$\begin{aligned} x_{Mi} &= x_M + v_x t_i \\ y_{Mi} &= y_M + v_y t_i \\ z_{Mi} &= z_M + v_z t_i \end{aligned} \tag{23}$$

Formulae (1), (2), and (3) should be replaced with:

$$\begin{aligned} TM_{ix} &= (x_{Mi} - x_T) \\ TM_{iy} &= (y_{Mi} - y_T) \\ TM_{iz} &= (z_{Mi} - z_T) \end{aligned} \tag{1'}$$

$$\begin{aligned} R_iM_{ix} &= (x_{Mi} - x_{Ri}) \\ R_iM_{iy} &= (y_{Mi} - y_{Ri}) \\ R_iM_{iz} &= (z_{Mi} - z_{Ri}) \end{aligned} \tag{2'}$$

$$Doppl_i = Doppl_{Ti} + Doppl_{Ri} \tag{3'}$$

In principle it is possible to use several Doppler and Doppler rate measurement of the same observer at different times.

4 A worked out example

During the Geminids 2009, the observers listed in Table 1 were recording `.wav` files, which allow the measurement of head echoes.

Figure 2 is a typical recording made with the Spectrum Lab freeware (DL4YHF, 2010). The descending lines lasting several minutes are mainly reflections caused by high level (10 km) planes within 30 km of the beacon.

The faint horizontal lines (e.g. at 740 and 840 Hz) are local interference. Normally the carrier is not directly detected in this particular setup.

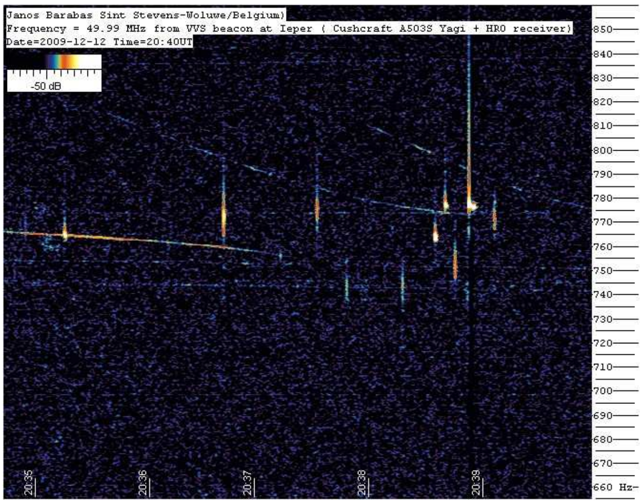

Figure 2 – Spectrumlab 5 minute recording of Janos Barabas during the Geminids 2009 maximum.

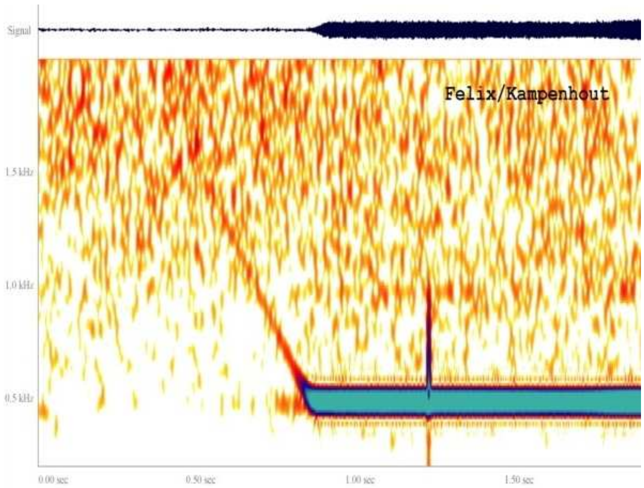

Figure 3 – Head echo of the 2009 December 12, 20^h38^m UT Geminid, as recorded by Felix Verbelen.

Twelve meteors are seen as 'vertical' streaks, clustering in the 730–800 Hz frequency band. As this recording was made during the maximum of the Geminids, there is a high probability that most of them are Geminids indeed. The sporadic activity during that time of the day (local evening) is normally low.

The Doppler spread is related to the thermal motion of the ions of the trails. The carrier frequency is near the midpoint of the vertical scale, at 770 to 775 Hz.

In the low time resolution Spectrum Lab recording of Figure 2 the trail at $20^h38^m50^s$ extends nearly vertical up to at least 840 Hz. Figure 3 shows the same meteor trail with a much greater time resolution as produced by the freeware program, Spectrogram by R.S. Horn (Electronics Lab, 2010). The increased time resolution of Spectrogram emphasizes the meteor is definitely a head echo swiftly approaching the point of closest approach for that observer's radio system.

Figure 4 is the compilation of all observed head echoes reduced to the same time and frequency scale. It is remarkable that the observer closest to the beacon (Table 3), Johan Coussens, did not record a sufficiently strong head echo.

Table 1 – Radio observers during the 2009 Geminids contributing to this work.

Name	Location (Belgium)	Longitude (E) dec degrees	Latitude (N) dec degrees	Antenna Altitude ASL (m)
VVS beacon at Astrolab-IRIS Zillebeke (Ypres)		2.9100	50.8180	41
Johan Coussens	Harelbeke	3.3293	50.8566	65
Dirk Van Hessche	Ninove	3.9868	50.8249	
Roger Segers	Puurs	4.2835	51.0709	
Roland Oeyen	Lembeek	4.1965	50.7152	63
Janos Barabas	Sint Stevens-Woluwe	4.4560	50.8760	
Felix Verbelen	Kampenhout	4.5944	50.9503	15
Willy Camps	Tessenderlo	5.0922	51.0822	26
Lucas Pellens	Overpelt	5.4324	51.2039	

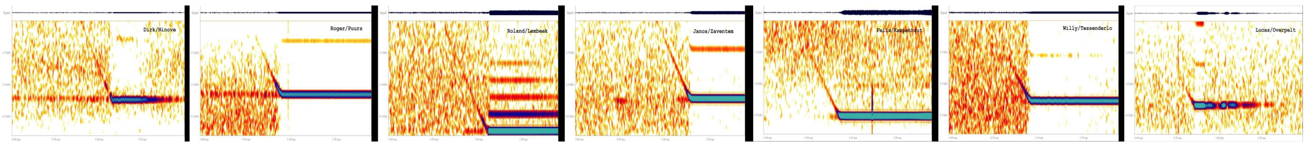

Figure 4 – Impression of the head echo of 2009 December 12, $20^{\mathrm{h}}38^{\mathrm{m}}$ UT by all observers.

Table 2 – Basic head echo data of the 2009 December 12, $20^{\mathrm{h}}38^{\mathrm{m}}$ UT Geminid, measured from observer's records.

head echo	200912122038							
Observer	location/Belgium	*t*1	*freq*1	*t*2	*freq*2	*zero-freq*	*slope* (Hz/sec)	*t_0-freq*
Johan Coussens	Harelbeke	no HE						
Dirk Van Hessche	Ninove	954	1449	1147	806	762	-3332	1160
Roger Segers	Puurs	694	1490	874	910	851	-3222	892
Roland Oeyen	Lembeek	648	1819	1062	414	274	-3394	1103
Janos Barabas	Zaventem	1074	1464	1236	932	780	-3284	1282
Felix Verbelen	Kampenhout	586	1290	810	614	488	-3018	852
Willy Camps	Tessenderlo	746	1165	876	814	729	-2700	907
Lucas Pellens	Overpelt	615	921	684	732	658	-2739	711

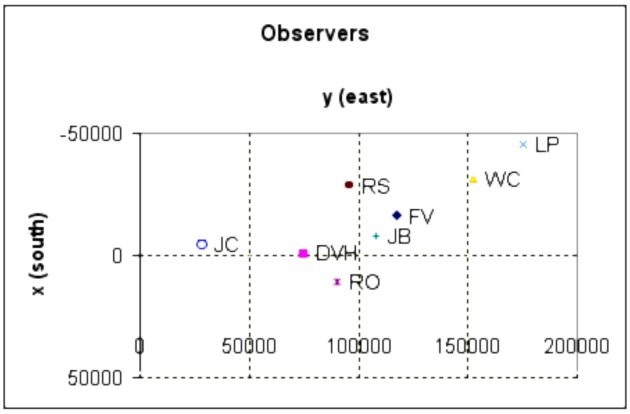

Figure 5 – Location of the observers with respect to the transmitter in the origin.

Two points, $t1$ and $t2$, in Table 2 are measured as far apart as possible on the trail. The values are in milliseconds. Times are NTP synchronized every hour with a tool such as DIMENSION 4 (Thinking Man Software, 2010).

The base line frequency *zero-freq* and the corresponding time *t_0-freq* are also measured, but are not used in the following calculations.

The slope of the head echo Doppler is simply calculated as the chord between the two points:

$$slope = \frac{freq1 - freq2}{t1 - t2} \tag{24}$$

This is the best approximation for the slope at the mid of the interval $[t1, t2]$, or $(t1 + t2)/2$.

All formulae (1) to (23) are for a general Cartesian system. We choose now a more specific coordinate system that allows easier interpretation of the resulting positions and velocities:

- the transmitter is at the origin of the coordinate system,
- the x-axis is oriented to the local south of the transmitter (tangent to the Earth ellipsoid),
- the y-axis is oriented to the local east of the transmitter (tangent to the Earth ellipsoid),
- the z-axis complements the right handed system, and therefore is pointing to the local zenith.

The resulting Cartesian coordinates are found in Table 3, and the plot on the tangent (x, y) plane in Figure 5. Most observers are located in a sector north east to south east of the transmitter.

For our Geminid example we follow the 'alternative procedure' for stream meteors using formulae (20)–(22).

The position of the standard Geminids radiant $\alpha = 113°$, $\delta = +32°$ in horizontal coordinates at the location of the beacon is: azimuth $Az = 257°$, elevation $h = 34°$, and the components v_x, v_y, v_z of the velocity vector for meteor speed $v = 34400$ m/s:

$$\begin{aligned} v_x &= -\cos(Az)\cos(h)v \\ v_y &= \sin(Az)\cos(h)v \\ v_z &= -\sin(h)v \end{aligned} \tag{25}$$

giving numerical values:

$$\overline{v} = (6415.4, -27788.0, -19236.2) \tag{26}$$

A logical starting value for (x_M, y_M, z_M) is $(0, 0, 90000)$, or 90 km above the beacon. The downhill simplex method minimizing $J + \lambda J'$ (22) finds an optimal point (rounded to the whole km) at $(-22000, 9000, 960000)$. The weight factor λ in (22) was chosen to be 0.2.

We choose $(x_M, y_M, z_M) = (-16000, 18000, 96000)$, for which following detailed calculations are performed.

This is the position along the trail at time t = 0. This is well before the start of the observed head echo.

The corresponding x_{Mi}, y_{Mi}, z_{Mi} for the mid point of the measured head echoes are according to (23):

Observer	ti	x	y	z
Verbelen	0.698	−17522	−10396	82573
Van Hessche	1.051	−15261	−20191	75792
Camps	0.811	−16797	−13536	80399
Pellens	0.650	−17833	−9048	83506
Oeyen	0.855	−16515	−14759	79553
Segers	0.784	−16970	−12786	80919
Barabas	1.155	−14590	−23095	73782

The z-values at these midpoints of the head echo are realistic.

The resulting errors are according to (20) and (21):

Observer	(O − C)dD/dt	(O − C)$Doppl$
Verbelen	−125.2	−191.2
Van Hessche	309.9	−227.5
Camps	6.2	499.8
Pellens	−307.4	277.5
Oeyen	−86.0	−151.2
Segers	−57.2	−407.1
Barabas	41.7	956.8

These errors are on the high side, especially the Doppler differences. This was only the initial step for a chosen x_M, y_M, z_M. The errors can still be reduced with the iterative procedure yet they remain rather high, mainly due to timing errors. A small timing error has a large impact on the instantaneous Doppler due to the high Doppler rate.

As there is only limited redundancy in the measurements we did not try to identify an outlier. Instead we made Monte Carlo simulations for the timing errors. Each timing instance was subjected to a 5 ms standard deviation.

The resulting horizontal plane scatter graph (Figure 6) shows a large spread in the north-south direction. The large spread is the result of the direction of the meteor in combination with the location of the observers.

The height scatter turns out to be much more limited, and there is only a slight dependency between z and both x and y.

It is unclear why Johan Coussens did not record the head echo. Probably the signal was too weak compared to the strong directly received carrier. Another possibility is that there is a selectivity effect at play.

General procedure (20), which determines both the meteor position and velocity, was tried with insufficient

Table 3 – Cartesian coordinates of the observers with respect to the transmitter.

	x	y	z	r
Beacon	0.0	0.0	0.0	0.0
Johan Coussens (JC)	−4148.1	28822.7	−1.3	29119.6
Dirk Van Hessche (DVH)	−1085.3	75164.5	−427.1	75173.6
Roger Segers (RS)	−28793.4	95559.9	−779.5	99806.6
Roland Oeyen (RO)	10882.3	90146.5	−582.1	90802.8
Janos Barabas (JB)	−7353.0	108098.2	−918.5	108351.9
Felix Verbelen (FV)	−15831.4	117647.7	−1087.6	118713.1
Willy Camps (WC)	−31405.6	152178.5	−1863.4	155396.5
Lucas Pellens (LP)	−45689.6	175533.6	−2574.8	181400.7

results for this example. The subject will be pursued when more accurate data are available.

5 Conclusion / future

The full theory for determining meteor trajectories from multiple Doppler head echo observations has been established.

Numerical results are encouraging, but will only be truly valuable if the timing accuracy of the recordings is improved to a few milliseconds.

Additional observing stations spread around the transmitter would improve the geometry and contribute to better results.

Several simultaneous head echoes are recorded per day. The identification, measurements and calculations of head echoes are currently done manually therefore the analysis procedure is very time intensive. A method to automate the analysis is needed to cope with the high volume of data.

Acknowledgments

We wish to thank:

- Astrolab IRIS for hosting the beacon and the VVS sponsoring the project and yearly license,
- Jeff Brower for greatly improving this text,
- Eddy Jespers (Eclips) for importing the MRX-50 receivers,
- Enric Algeciras for organizing the CE compliance tests of the MRX-50 receivers,
- Belgian Institute for Postal Services and Telecommunications (BIPT) for allocating the beacon frequency,
- Masa-Yuki Yamamoto for his invaluable liaison role with AITEC,
- David Entwistle for the interesting discussions about the Monte Carlo method and sensitivity analysis, and thoroughly checking the calculations.

References

AMRO (2010). “The international project for radio meteor observation”. `http://www.amro-net.jp/english/hro.htm` .

DL4YHF (2010). “DL4YHF’s amateur radio software: Audio spectrum analyzer (Spectrum Lab)”. `http://www.qsl.net/dl4yhf/spectra1.html`.

Electronics Lab (2010). “Spectrogram”. `http://www.electronics-lab.com/downloads/pc/003/index.html`, `http://www.dk3red.homepage.t-online.de/en/s11.htm#b1`.

Manning L. A., Villard, Jr. O. G., and Peterson A. M. (1949). “Radio Doppler investigation of meteoric heights and velocities”. *Journal of Applied Physics*, **20**, 475–479.

Richardson J. and Kuneth W. (1998). “Revisiting the Radio Doppler effect for forward-scatter meteor head echoes”. *WGN, Journal of the IMO*, **26**, 117–130.

Steyaert C. (2006). “The VVS meteor beacon”. In Bastiaens L., Verbert J., Wislez J.-M., and Verbeeck C., editors, *Proceedings of the International Meteor Conference, Oostmalle, Belgium, 15-18 September, 2005*, pages 25–33.

Steyaert C., Brower J., and Verbelen F. (2006). “A numerical method to aid in the combined determination of stream activity and observability function”. *WGN, Journal of the IMO*, **34**, 87–93.

Steyaert C. and Verbelen F. (2006). “1 jaar VVS meteoorbaken: resultaten en mogelijkheden”. (Presentation VVS Weekend 2006).

Thinking Man Software (2010). “Dimension 4 v5.0”. `http://www.thinkman.com/dimension4` .

Handling Editor: Javor Kac

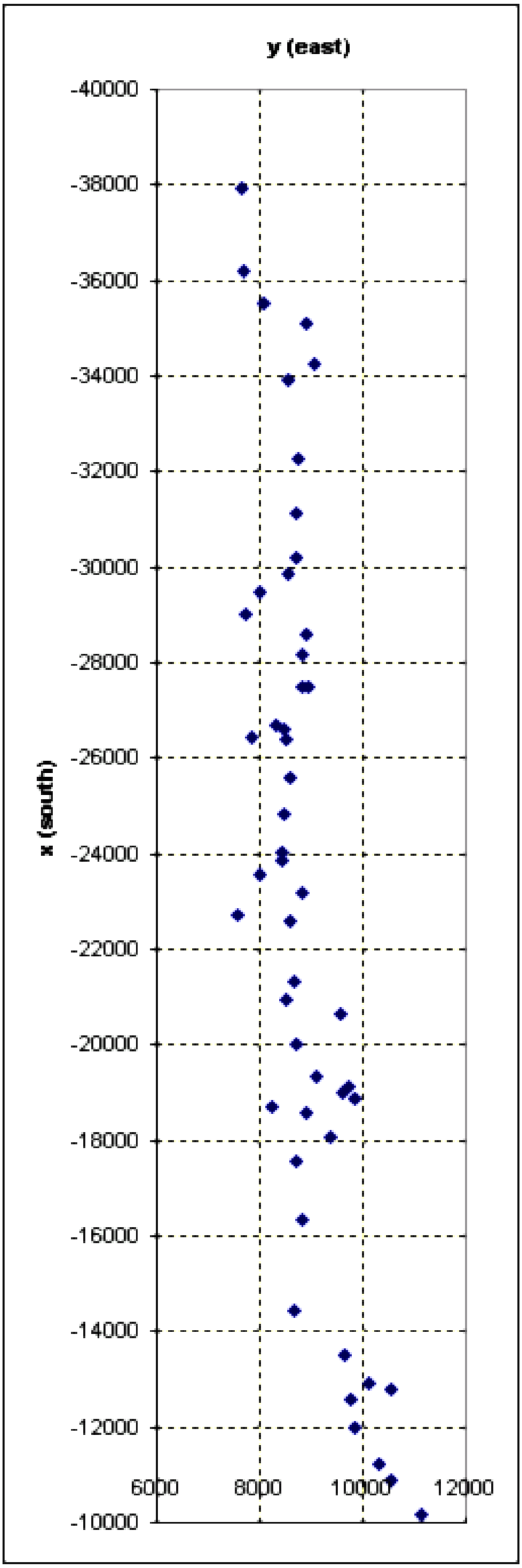

Figure 6 – Scatter on the results for the Monte Carlo simulation: horizontal plane.

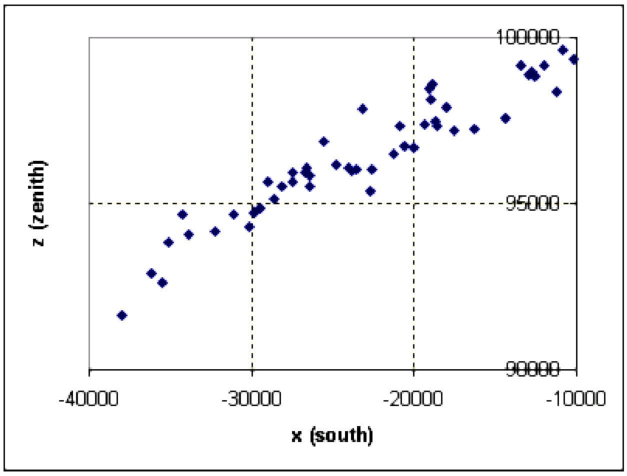

Figure 7 – Scatter on the results for the Monte Carlo simulation: north-south vertical plane.

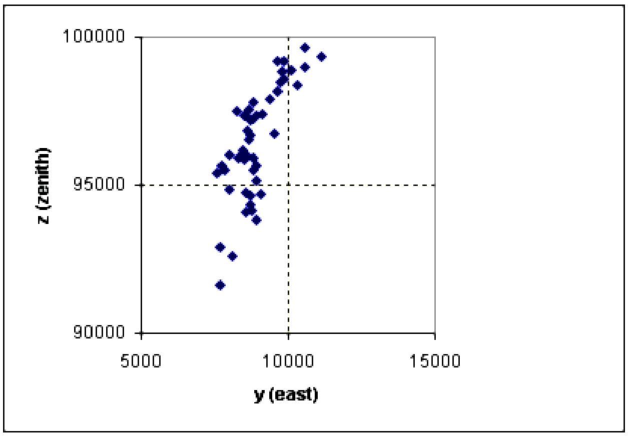

Figure 8 – Scatter on the results for the Monte Carlo simulation: east-west vertical plane.